Simulation of Power Heterojunction Bipolar Transistors on Gallium Arsenide

Vassil Palankovski, Ruediger Schultheis, and Siegfried Selberherr, *Fellow, IEEE*

***Abstract*—We demonstrate the results of two-dimensional (2-D) hydrodynamic simulations of one-finger power heterojunction bipolar transistors (HBTs) on GaAs. An overview of the physical models used and comparisons with experimental data are given.**

We present models for the thermal conductivity and the specific heat applicable to all relevant diamond and zinc-blende structure semiconductors. They are expressed as functions of the lattice temperature and, in the case of semiconductor alloys, of the material composition.

***Index Terms*—Electrothermal effects, heating, semiconductor device thermal factors, simulation software.**

I. Introduction

HETEROJUNCTION bipolar transistors (HBTs) attract much industrial interest because of their capability to operate at high current densities [1], [2]. AlGaAs/GaAs or InGaP/GaAs-based devices are promising candidates for power applications in modern mobile telecommunication systems.

Heat generated at the heterojunctions cannot completely leave the device, especially in the case of III-V semiconductor materials. Therefore, significant self-heating occurs in the device and leads to a change of the electrical device characteristics.

Accurate simulations save expensive technological efforts to obtain significant improvements of the device performance. The two-dimensional (2-D) device simulator MINIMOS-NT [3] is extended to deal with different complex materials and structures, such as binary and ternary semiconductor III-V alloys with arbitrary material composition profiles. Various important physical effects, such as bandgap narrowing, surface recombination, and self-heating, are taken into account.

This paper describes the physical models and gives examples of simulations verified by measurements.

II. The Physical Models

In previous work, we emphasized on bandgap narrowing as one of the crucial heavy-doping effects to be considered for bipolar devices [4]. We have developed a new physically-based analytical bandgap narrowing model, applicable to compound

Manuscript October 23, 2000. The review of this paper was arranged by Editor M. A. Shibib.

V. Palankovski and S. Selberherr are with Institut für Mikroelektronik, Technische Universität Wien, A-1040 Vienna, Austria.

R. Schultheis is with Infineon Technologies AG, Wireless Systems WS TI S MWP, D-81730 Munich, Germany.

Publisher Item Identifier S 0018-9383(01)04239-3.

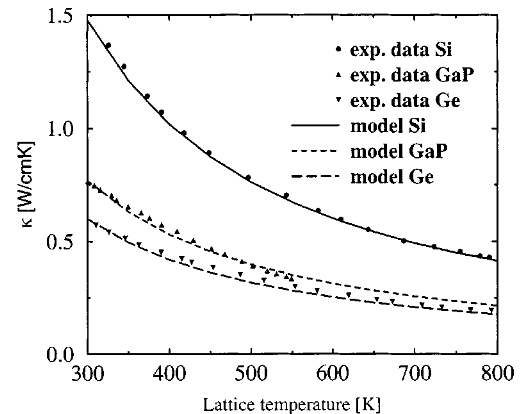

Fig. 1. Temperature dependence of the thermal conductivity. Comparison between experimental data and the model for Si, Ge, and GaP.

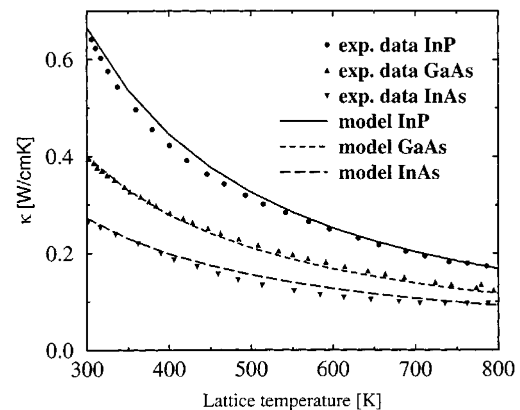

Fig. 2. Temperature dependence of the thermal conductivity. Comparison between experimental data and the model for InP, GaAs, and InAs.

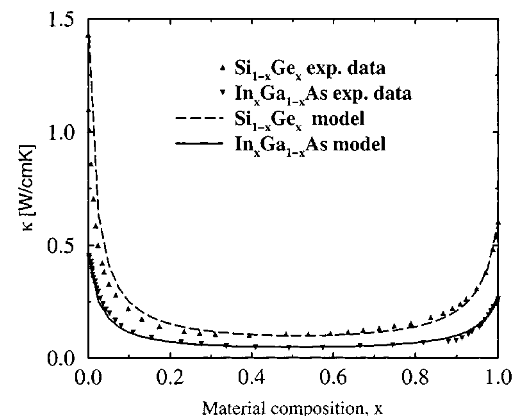

Fig. 3. Material composition dependence of the thermal conductivity. Comparison between experimental data and the model for SiGe and InGaAs.

0018–9383/01$10.00 © 2001 IEEE

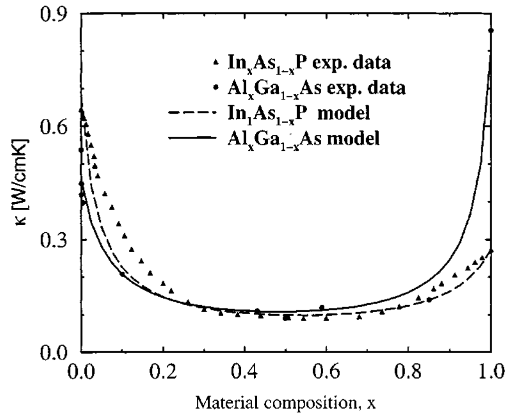

Fig. 4. Material composition dependence of the thermal conductivity. Comparison between experimental data and the model for InAsP and AlGaAs.

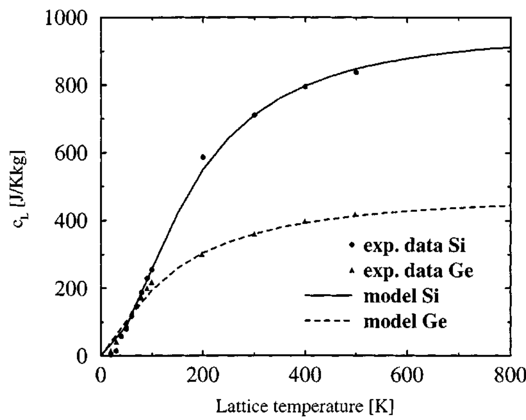

Fig. 5. Temperature dependence of the specific heat. Comparison between experimental data and the model for Si and Ge.

semiconductors, which accounts for the semiconductor material, the dopant species, and the lattice temperature. As the minority carrier mobility is of considerable importance for bipolar transistors, a new universal low field mobility model has been implemented in MINIMOS-NT [5]. It is based on Monte-Carlo simulation results and distinguishes between majority and minority electron mobilities.

Energy transport equations are necessary to account for nonlocal effects, such as velocity overshoot [6], [7]. In recent work, a new model for the electron energy relaxation time has been presented [8]. It is based on Monte-Carlo simulation results and is applicable to all relevant semiconductors with diamond and zinc-blende structure. The energy relaxation times are expressed as functions of the carrier and lattice temperatures and in the case of semiconductor alloys of the material composition.

Considering the nature of the simulated devices (including abrupt InGaP/GaAs and AlGaAs/InGaP heterointerfaces) and the high electron temperatures observed at maximum bias we use sophisticated thermionic-field emission interface models [9] in conjunction with the hydrodynamic transport model. At the other (homogeneous or graded) interfaces continuous quasi-Fermi levels were assumed.

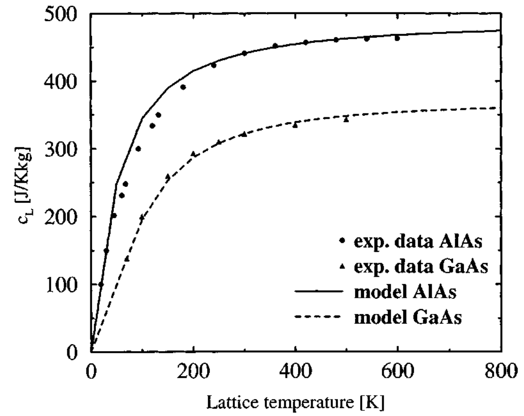

Fig. 6. Temperature dependence of the specific heat. Comparison between experimental data and the model for GaAs and AlAs.

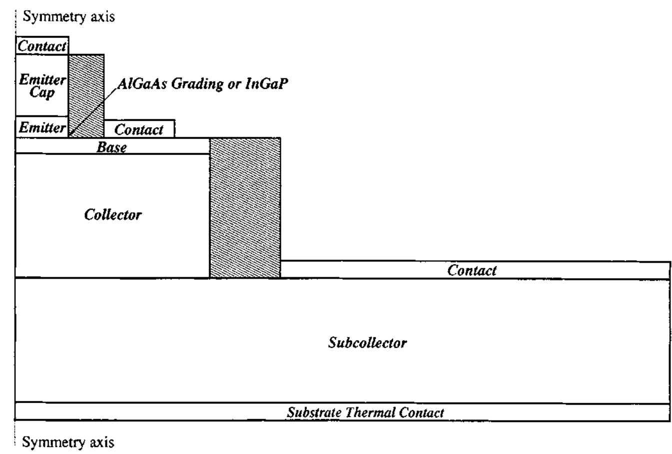

Fig. 7. Principal simulated HBT structure. The GaAs substrate is replaced by a thermal contact.

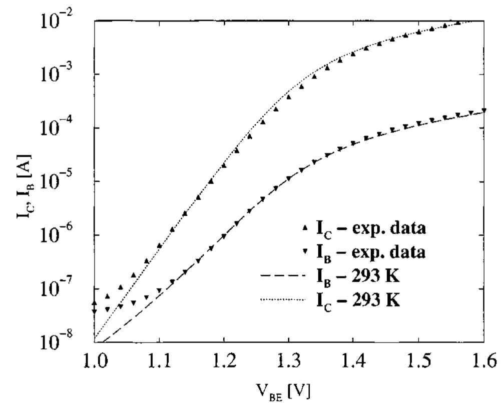

Fig. 8. Forward Gummel plots at $V_{CB} = 0$ V for Device 1. Comparison with measurement data.

III. Self-Heating Simulation

The 2-D device simulator MINIMOS-NT [3] accounts for self-heating effects by solving the lattice heat flow equation (1) self-consistently with the energy transport equations. Finally, a system of six partial differential equations is solved

$$\text{div}\,(\kappa_L \cdot \text{grad}T_L) = \rho_L \cdot c_L \cdot \frac{\partial T_L}{\partial t} - H \tag{1}$$

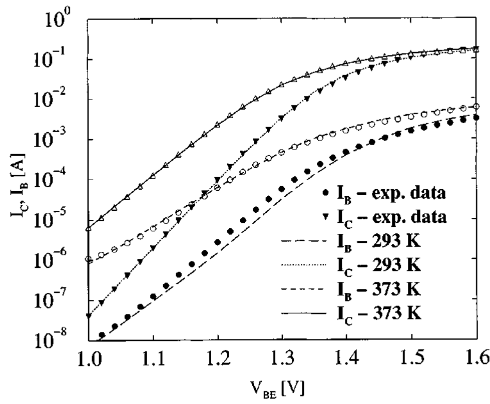

Fig. 9. Forward Gummel plots at $V_{CB} = 0$ V for Device 2. Comparison with measurement data at 293 K and 373 K.

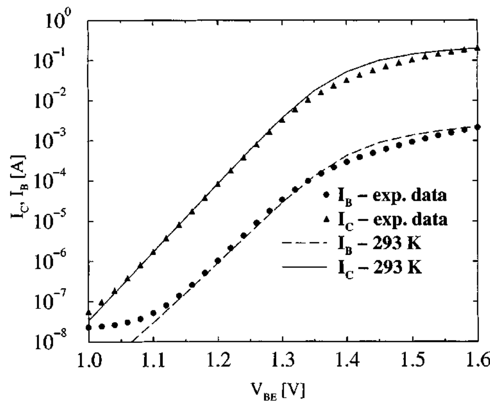

Fig. 10. Forward Gummel plots at $V_{CB} = 0$ V for Device 4. Comparison with measurement data.

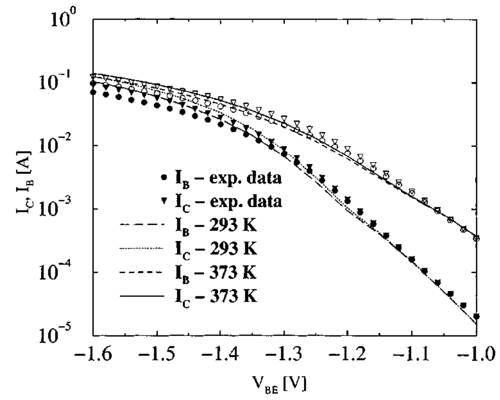

Fig. 11. Reverse Gummel plots $V_{CB} = 0$ V for Device 4. Comparison with measurement data at 293 K and 373 K.

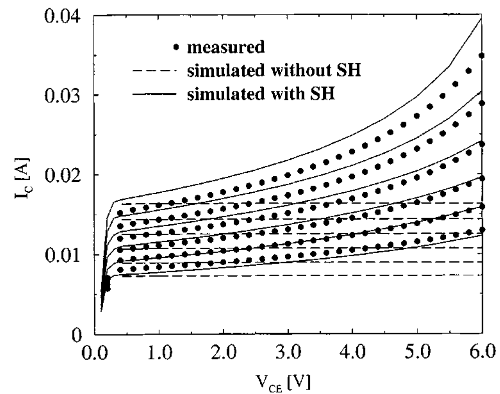

Fig. 12. Output characteristics for Device 3. Simulation with and without self-heating compared to measurement data.

where

T_{L}	lattice temperature;
t	time variable;
H	heat generation term;
ρ_{L}, c_{L}, and κ_{L}	material's mass density, specific heat, and thermal conductivity, respectively.

For different semiconductor materials proper models must be used.

A. Mass Density Models

The values of the mass density of the basic semiconductor materials are well known, and are used to model the values for compound materials. In the case of SiGe and ternary III-V alloys, it is expressed by a linear change between the values of the basic materials A and B

$$\rho^{\mathrm{AB}} = (1-x)\cdot\rho^{\mathrm{A}} + x\cdot\rho^{\mathrm{B}}. \tag{2}$$

The parameter values used in MINIMOS-NT are summarized in Table I.

B. Thermal Conductivity

The temperature dependence of κ_L of the basic semiconductor materials is modeled by a simple power law

$$\kappa_{\mathrm{L}}(T_{\mathrm{L}}) = \kappa_{300}\cdot\left(\frac{T_{\mathrm{L}}}{300\ \mathrm{K}}\right)^{\alpha} \tag{3}$$

where κ_{300} is the value for the thermal conductivity at 300 K. This approximation is in good agreement with experimental data [10]–[13], as presented in Figs. 1 and 2, where comparisons between experimental data and the results obtained with our model are shown for the thermal conductivity in the temperature range 300 K–800 K. The parameter values used are summarized in Table II.

In the case of alloy materials $\mathrm{A}_{1-x}\mathrm{B}_x$, κ_L varies between the values of the basic materials (A and B). A harmonic mean is used to model κ_{300}. An additional bowing factor C is introduced in order to account for the drastic reduction of the thermal conductivity with the increase of material composition x. The temperature dependence factor α is linearly interpolated because of lack of experimental data at temperatures other than 300 K

$$\kappa_{300}^{\mathrm{AB}} = \frac{1}{\left(\dfrac{1-x}{\kappa_{300}^{\mathrm{A}}} + \dfrac{x}{\kappa_{300}^{\mathrm{B}}} + \dfrac{(1-x)\cdot x}{C}\right)} \tag{4}$$

$$\alpha^{\mathrm{AB}} = (1-x)\cdot\alpha^{\mathrm{A}} + x\cdot\alpha^{\mathrm{B}}. \tag{5}$$

The parameter values used in MINIMOS-NT are summarized in Table III.

In Figs. 3 and 4, comparisons between experimental data from [11]–[16] and the results obtained with our model are shown for the thermal conductivity at 300 K.

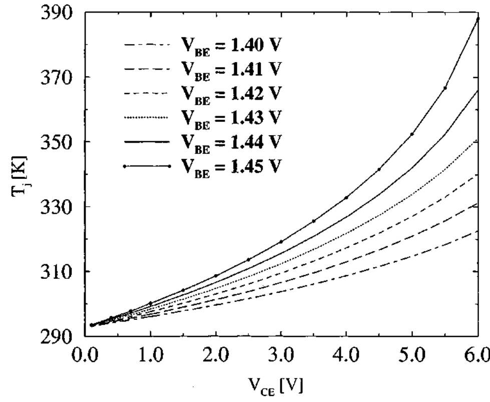

Fig. 13. Intrinsic device temperature versus V_{CE} for Device 3.

TABLE I
PARAMETER VALUES FOR MASS DENSITY

Material	ρ [g/cm^3]
Si	2.33
Ge	5.327
GaAs	5.32
AlAs	3.76
InAs	5.667
InP	4.81
GaP	4.138

TABLE II
PARAMETER VALUES FOR THERMAL CONDUCTIVITY

Material	κ_{300} [W/K m]	α
Si	148	-1.65
Ge	60	-1.25
GaAs	46	-1.25
AlAs	80	-1.37
InAs	27.3	-1.1
InP	68	-1.4
GaP	77	-1.4

C. Specific Heat

The specific heat capacity c_{L} of the considered material is modeled with

$$c_{\mathrm{L}}(T_{\mathrm{L}}) = c_{300} + c_1 \cdot \frac{\left(\dfrac{T_{\mathrm{L}}}{300\ \mathrm{K}}\right)^{\beta} - 1}{\left(\dfrac{T_{\mathrm{L}}}{300\ \mathrm{K}}\right)^{\beta} + \dfrac{c_1}{c_{300}}}. \quad (6)$$

where c_{300} is the value for the specific heat at 300 K [17]. The model is used for the basic semiconductor materials. In Figs. 5 and 6, we present comparisons between experimental data and the results obtained with our model for the specific heat. Note the excellent agreement it gives in a wide temperature range (0 K–800 K). The parameter values used are summarized in Table IV.

TABLE III
PARAMETER VALUES FOR THERMAL CONDUCTIVITY

Material	C [W/K m]
SiGe	2.8
AlGaAs	3.3
InGaAs	1.4
InAlAs	3.3
InAsP	3.3
GaAsP	1.4
InGaP	1.4

TABLE IV
PARAMETER VALUES FOR THE SPECIFIC HEAT

Material	c_{300} [J/K kg]	c_1 [J/K kg]	β
Si	711	255	1.85
Ge	360	130	1.3
GaAs	322	50	1.6
AlAs	441	50	1.2
InAs	394	50	1.95
InP	410	50	2.05
GaP	519	50	2.6

The specific heat capacity coefficients in the case of SiGe and ternary III-V compounds are expressed by a linear change between the values of the basic materials (A and B)

$$c_{\mathrm{L}}^{\mathrm{AB}} = (1-x) \cdot c_{\mathrm{L}}^{\mathrm{A}} + x \cdot c_{\mathrm{L}}^{\mathrm{B}}. \quad (7)$$

IV. FABRICATION OF THE SIMULATED DEVICES

The electrical behavior of four different types of one-finger power HBTs with emitter area of $3 \times 30\ \mu\mathrm{m}^2$ has been studied at several ambient temperatures. Typical operating temperatures for the devices under consideration range from 300 K to 380 K [2]. All devices are MOCVD epitaxially grown. The first device, later on referred to as Device 1, has the following layer sequence. The cap is formed by an n^+-InGaAs/n-GaAs layer. The emitter consists of 80 nm Si-doped n-$Al_{0.28}Ga_{0.72}As$ with 20-nm graded layers on its top and bottom, respectively. The 120-nm GaAs base is carbon doped ($p^+ = 3.10^{19}$ cm^{-3}), followed by 700-nm GaAs collector ($n^- = 2.10^{16}$ cm^{-3}) and 700-nm GaAs subcollector ($n^+ = 5.10^{18}$ cm^{-3}). In two other devices (Device 2 and Device 3) the graded AlGaAs layer next to the base-to-emitter junction has been replaced by a 20-nm InGaP ledge layer (n= 4.10^{17} cm^{-3} and 3.10^{17} cm^{-3}, respectively). Both devices differ in the base carbon doping ($p^+ = 3.10^{19}$ cm^{-3} versus 4.10^{19} cm^{-3}) and layer thickness (80 nm versus 120 nm). A state-of-the-art 40-nm InGaP emitter (n= 4.10^{19} cm^{-3}) HBT with a 120-nm thick base is the last device type under consideration (Device 4). All HBTs are processed by

etching a double mesa structure and passivated by Si_3N_4. The simulated device structure is shown in Fig. 7.

V. Simulation Results

One concise set of model parameters was used in all simulations. The extrinsic parasitics, e.g., the emitter interconnect resistance, were accounted for in the simulation by adding resistance of 1 Ω at all electric contacts. In Fig. 8, we present the simulated forward Gummel plot for Device 1 at 293 K compared to experimental data. We achieve good agreement at moderate and high voltages, typical for operation of this kind of devices.

Encouraging results for Device 2 have also been achieved. In Fig. 9, we include the simulated Gummel plot at 373 K to demonstrate our ability to reproduce correctly the thermal device behavior. Comparisons with measured data for Device 4 are shown in Figs. 10 and 11. Note the very good agreement for the reverse Gummel plots also at higher temperatures.

The results verify our models and therefore are a good prerequisite for simulation of self-heating effects. For that purpose, an additional, substrate thermal contact has been introduced. A measured value of about 400 K/W for the thermal resistance has been used [19]. The thermal dissipation through the emitter and base contacts is assumed to be negligible, therefore, a Neumann boundary condition was assumed.

In the case of simulation of the output HBT characteristics one meets severe problems to achieve realistic results, especially in the case of power devices, which is the case with the HBTs considered in this work. As stated in [20], as collector-to-emitter voltage V_{CE} increases, the power dissipation increases, gradually elevating the junction temperature above the ambient temperature. This leads to gradually decreasing collector currents I_C at constant applied base current I_B or, respectively, gradually increasing I_C at constant base-to-emitter voltage V_{BE}. In Fig. 12, we show the simulated output device characteristics compared to measurements for constant $V_{BE} = 1.4$ V to 1.45 V using a 0.01 V step. We achieve good agreement in the simulation with self-heating effects included. In Fig. 13, we present the intrinsic temperature in the device depending on the V_{CE}. For Device 3, the temperature reaches as much as 400 K for the specified thermal resistance. As we already stated in [21], such lattice temperatures significantly change the material properties of the device and, therefore, its electrical characteristics. This confirms the necessity of exact dc simulations at several high ambient temperatures before including self-heating effects.

VI. Conclusions

We presented simulations of power HBTs on GaAs. New thermal models were employed to get good agreement with experimental results and aid getting an insight and understanding of the real device and thus achieve better device performance. Thermal models for semiconductor device simulation valid in wide temperature range for various HBTs investigated experimentally were tuned to include self-heating effects in the device.

Appendix

The parameter values used in MINIMOS-NT are summarized in Tables I-IV.

Acknowledgment

The authors acknowledge Dr. W. Kellner from Infineon Technologies AG, Corporate Research (CPR C), and Dr. P. Zwicknagl from Infineon Technologies AG, Semiconductor Group (GS PE HT 1), for support and valuable input to this work. V. Palankovski thanks Dr. T. Grasser for his excellent work on MINIMOS-NT and for valuable discussions on thermal problems.

References

[1] J. E. Müller, P. Baureis, O. Berger, T. Boettner, N. Bovolon, R. Schultheis, G. Packeiser, and P. Zwicknagl, "A small chip size 2 W, 62% efficient HBT MMIC for 3 V PCN applications," *IEEE J. Solid-State Circuits*, vol. 33, pp. 1277–1283, Sept. 1998.

[2] R. Schultheis, N. Bovolon, J.-E. Müller, and P. Zwicknagl, "Electrothermal modeling of heterojunction bipolar transistors (HBTs)," in *Proc. 11th III-V Semiconductor Device Simulation Workshop*, Lille, France, May 1999.

[3] T. Binder, K. Dragosits, T. Grasser, R. Klima, M. Knaipp, H. Kosina, R. Mlekus, V. Palankovski, M. Rottinger, G. Schrom, S. Selberherr, and M. Stockinger, *MINIMOS-NT User's Guide*: Institut für Mikroelektronik, 1998.

[4] V. Palankovski, G. Kaiblinger-Grujin, H. Kosina, and S. Selberherr, "A dopant-dependent bandgap narrowing model application for bipolar device simulation," in *Simulation of Semiconductor Processes and Devices*, K. D. Meyer and S. Biesemans, Eds. New York: Springer-Verlag, 1998, pp. 105–108.

[5] V. Palankovski, G. Kaiblinger-Grujin, and S. Selberherr, "Implications of dopant-dependent low-field mobility and bandgap narrowing on the bipolar device performance," *J. Phys. IV*, vol. 8, pp. 91–94, 1998.

[6] B. Neinhüs, P. Graf, S. Decker, and B. Meinerzhagen, "Examination of transient drift-diffusion and hydrodynamic modeling accuracy for SiGe HBTs by 2D Monte-Carlo device simulations," in *27th Eur. Solid-State Device Research Conf.*, H. Grünbacher, Ed., 1997, pp. 188–191.

[7] T. Kumar, M. Cahay, and K. Roenker, "Ensemble Monte Carlo analysis of self-heating effects in graded heterojunction bipolar transistors," *J. Appl. Phys.*, vol. 83, no. 4, pp. 1869–1877, 1998.

[8] V. Palankovski, B. Gonzales, H. Kosina, A. Hernandez, and S. Selberherr, "A new analytical energy relaxation time model for device simulation," in *Proc. 2nd Int. Conf. Modeling and Simulation of Microsystems*, 1999, pp. 395–398.

[9] D. Schroeder, *Modeling of Interface Carrier Transport for Device Simulation*. New York: Springer-Verlag, 1994.

[10] J. A. King, *Material Handbook for Hybrid Microelectronics*. Norwood, MA: Artech House, 1988.

[11] P. D. Maycock, "Thermal conductivity of silicon, germanium, III-V compounds and III-V alloys," *Solid-State Electron.*, vol. 10, pp. 161–168, 1967.

[12] M. Landolt and J. Börnstein, *Numerical Data and Functional Relationships in Science and Technology, vol. 22/A of New Series, Group III*. New York: Springer-Verlag, 1987.

[13] A. Katz, *Indium Phosphide and Related Materials*. Norwood, MA: Artech House, 1992.

[14] S. Adachi, *Physical Properties of III-V Semiconductor Compounds*. New York: Wiley, 1992.

[15] ——, Properties of Aluminum Gallium Arsenide, IEE INSPEC, 1993.

[16] P. Bhattacharya, Properties of Lattice-Matched and Strained Indium Gallium Arsenide, IEE INSPEC, 1993.

[17] S. Tiwari, *Compound Semiconductor Device Physics*. New York: Academic, 1992.

[18] M. Knaipp, "Modellierung von Temperatureinflüssen in Halbleiterbauelementen," Dissertation, Tech. Univ. Wien, Austria, 1998.

[19] N. Bovolon, P. Baureis, J.-E. Müller, P. Zwicknagl, R. Schultheis, and E. Zanoni, "A simple method for the thermal resistance measurement of AlGaAs/GaAs heterojunction bipolar transistors," *IEEE Trans. Electron Devices*, vol. 45, pp. 1846–1848, Aug. 1998.

[20] W. Liu, *Fundamentals of III-V Devices*. New York: Wiley, 1999.

[21] V. Palankovski, S. Selberherr, and R. Schultheis, "Simulation of heterojunction bipolar transistors on Gallium-Arsenide," in *Simulation of Semiconductor Processes and Devices*. Kyoto, Japan: Bus. Ctr. Acad. Soc. Jpn., 1999, pp. 227–230.

Vassil Palankovski was born in Sofia, Bulgaria, in 1969. He received the diploma degree in electrical engineering from the Technical University of Sofia in 1993, and the Ph.D. degree from the Institut für Mikroelektronik at the Technische Universität Wien, Austria, in 2000.

In 1997, after having worked for three years in the telecommunications field, he joined the Institut für Mikroelektronik at the Technische Universität Wien. In Summer 2000, he held a visiting research position at LSI Logic, Milpitas, CA. His scientific interests include device and circuit simulation, heterostructure device modeling, and physical aspects in general.

Rüdiger Schultheis was born in Fulda, Germany, in 1965. He received the Dipl.Ing. degree from the Technical University of Darmstadt, Germany, in 1991, and the Dr.-Ing. degree from the High Frequency Institute of the same university in 1996.

At the Technical University of Darmstadt, he was engaged in the development and 3-D electromagnetic simulation of high-frequency electrodes for both detection and deflection of heavy ion particle beams. In 1996, he joined the III-V Electronic Department of Siemens Corporate Research and Technology, Munich, Germany (now Infineon Technologies, Corporate Research CPR). Since that time, his work has been focussed on HBTs with respect to modeling, reliability, and circuit design.

Siegfried Selberherr (M'79–SM'84–F'93) was born in Klosterneuburg, Austria, in 1955. He received the Diplomingenieur degree in electrical engineering and the Ph.D. degree in technical sciences from the Technische Universität Wien, Austria, in 1978 and 1981, respectively.

Since 1984, he has been holding the "venia docendi" on "computer-aided design." Since 1988, he has been the head of the Institut für Mikroelektronik and since 1999 he has been Dean of the Fakultät für Elektrotechnik at the Technische Universität Wien. His current topics are modeling and simulation of problems for microelectronics engineering.